Robotica (2009) volume 27, pp. 303–310. © 2008 Cambridge University Press
doi:10.1017/S0263574708004773 Printed in the United Kingdom

Smart wheelchair perception using odometry, ultrasound sensors, and camera

O. Horn* and M. Kreutner

Laboratoire d'Automatique des Systèmes Coopératifs (L.A.S.C.), 7 rue Marconi, 57070 METZ, France.

(Received in Final Form: May 9, 2008. First published online: June 23, 2008)

SUMMARY
This paper deals with the perception mode of smart wheelchairs. First we evoke the many mobility aid prototypes developed in rehabilitation robotics by considering the point of view of perception. Then we describe the localization mode of the VAHM**. We show how the odometric, ultrasound, and vision sensors are used in a complementary way in order to locate the wheelchair in its known environment. The mode of adjustment of the odometric position by the least-squared method using ultrasonic measurements is detailed. Then the use of vision to perceive the vertical segments of the environment so as to refine the orientation is presented. The results of the tests carried out on the wheelchair are given and commented.

KEYWORDS: Smart wheelchair; Localization; Ultrasonic sensors; Vision

1. Introduction

During the last 15 years, the mobility aid for people with severe motor disabilities became a new field of research in mobile robotics. To that end, powered wheelchairs are designed by integrating an on-board computer that partially deals with the steering task. The implementation of such devices entails approaching the classic problems of mobile robotics (path planning, navigation, localization, etc.) and adapting them to the particular context of the application.

The VAHM project, developed in our laboratory, aims to conceive such a prototype. The vehicle is fitted with odometric, ultrasound, and vision sensors; in this paper we deal with its localization mode during movement. We endeavor to show how the specificity of the application led us to use the various sensors in a complementary way so as to make the most of measurements of the ones to make up for the weaknesses of the others.

The paper is organized as follows: In Section 2, we describe the works on similar projects developed by other teams. Section 3 shows the localization mode of the VAHM and the study on the validity of odometric measurements. Section 4 describes the approach on how to correct the position with the ultrasonic sensors, by using the least-squared method. Section 5 deals with orientation adjustment using pictures acquired by the camera. Finally we conclude by considering the contribution of this work on future developments of smart wheelchairs.

* Corresponding author. E-mail: horn@lasc.univ-metz.fr.
VAHM is the French acronym for autonomous vehicle for people with disabilities.

2. Previous Works

Several studies have been carried out to design smart wheelchairs. They led to systems with different levels of autonomy as well as different means of achieving various functionalities. One can count more than 20 prototypes which offer a diversity of movement approaches with various corresponding functionalities of perception. The referenced works are described according to their environment perception modes.

2.1. Reactive mode

Measurements are interpreted immediately to adapt the trajectory. The most prevalent method is "obstacle avoidance," which consists in modifying the trajectory to avoid colliding with an obstacle. This function may be achieved through various levels of interpretation of the measurements.

The most immediate approaches take measurements and reduce the speed in the direction where an obstacle is perceived, for example with ultrasound (US) measurements[1] or infrared (IR) measurements[28] or by combining IR, US, and bumper.[2–4] The whole US measurements can be gathered in a single representation allowing to choose the direction which is the closest to the one pointed out by the user and presenting no obstacle.[6,7] Obstacle avoidance can also be complementary to localization.[8] Other methods translate sensor readings into control on the motors for the avoidance of obstacle by resorting to fuzzy logic,[9–11] artificial intelligence,[12] or probabilistic models.[13,14]

Other reactive primitives take place directly from the sensor measurements using alternatives to obstacle avoidance. "Path following" will react to the sensor measurements by reproducing a trajectory learned during a training phase.[25,26] "Mobile following" makes the wheelchair carry out the same movement as a person or another vehicle as perceived by the camera.[1,9] "Wall following" consists in adjusting the trajectory on a line parallel with a wall, with the distance between the wheelchair and the wall measured by sonar sensors and kept constant.[7,10] And "door passing" slows the wheelchair down to make it move through a difficult crossing.[7,12]

2.2. Localization

Sensor measurements are used to establish the position of the wheelchair so as to carry out programmed trajectories correctly. The approaches differ depending on whether artificial beacons are present or not, on whether there is preliminary knowledge of the environment or not, and on the mode of interpretation of the measurements.

The position can be determined from a simple comparison between current data and learned data, which may be of various types: trajectories,[15] multidimensional histograms (color gradient textures, etc.),[17] or profiles of free space.[16]

The perception of known visual beacons is also possible. They can consist of a simple marking on the floor[18] or more or less complex patterns on the walls.[8,19]

Some works use more elaborate mathematical formalisms in order to adjust the odometric position. The measurements are matched with the features of the environment that they perceive. Then an adjustment of the position is worked out using the least-squared method[20,21,22,23] or a Kalman filter.[8,24]

3. Localization Approach

3.1. Presentation of the VAHM project

The VAHM project aims at developing a powered wheelchair dedicated to moving in an indoor environment. It offers the user various functionalities to make its driving easier. The prototype on which we work is shown in Fig. 1.

It consists of a classical Power Push™ powered wheelchair fitted with 16 ultrasonic sensors, an odometric system, a CCD camera fixed below the armrests, and a microcomputer. The man–machine communication system consists of a screen, on which the machine displays its information and requests, and of a sensor allowing the user to give his instructions.

The type and the activation means of the control handle depend on the abilities of the user. It can consist of a joystick, like on a standard powered wheelchair, or of an on-off switch, thanks to which the driver selects destinations displayed on the screen.[20] The on-board computer is intended for the realization of various functionalities, which may range from reactive primitives to the machine exerting full control of movements. In this case the user indicates the place he wants to reach, using the graphical interface, and the system looks for the best path and checks its achievement.

In this context the localization is essential in order to check that the trajectory is followed properly and that the destination is actually reached. Two distinct modes of localization are established according to the state of the wheelchair: stationary or moving. We developed a method based on the occupancy grids for the stationary wheelchair.[27] It allows to compute the position of the wheelchair from the ultrasonic measurements in less than one minute. When the wheelchair is moving, real-time execution requires a faster procedure which uses odometric measurements, ultrasonic measurements, and the pictures delivered by camera.

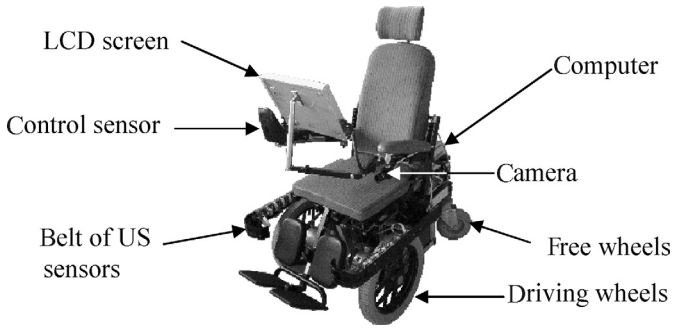

Fig. 1. Prototype of the VAHM.

We conceived two distinct procedures in order to make the most of the possibilities of each case. In fact, the static mode of localization requires few measurements but a significant processing time while the dynamic localization mode—which is the subject of this paper—uses more measurements but a shorter processing time.

The conception of the dynamic localization method is led by the search for the best complementarity between the perception abilities of our three sensors. Its principle is as follows: the odometry gives a first estimate of the position and orientation of the vehicle, then the ultrasonic measurements allow to adjust the position, and finally the orientation is refined by the camera. This principle is based on the following considerations:

- The odometric position is instantaneously delivered but is prone to drifting.
- The ultrasonic sensors give a first exteroceptive perception to correct the odometric drift but their orientation acuity is low because of their emission cone.
- The pictures allow to quickly specify the orientation of the vehicle if its position is known.

We will detail the various elements of this procedure and the results obtained during the tests on our prototype.

3.2. Principle of the odometry

The odometric position of the wheelchair is assessed by computing its move from a known starting point. This move is obtained thanks to the optical encoders, which measure the number of turns carried out by the wheels. The uncertainty on the diameter of the wheels and their possible skidding may cause errors on the computed position and the odometric position becomes more inaccurate as the traveled distance increases.

Studies have been carried out to assess these errors and to consider how best to overcome them[5]; the tested vehicles were robots with solid wheels. The wheelchair on which we work is equipped with air-inflated tires, so as to make the user acceptably comfortable; therefore, the diameter of the wheels can vary leading to more inaccuracies on the odometric position. That is why we have tested the accuracy of odometric data in our context.

3.3. Odometry testing on the prototype

The vehicle performed a rectilinear displacement of 1.50 m several times and we compared the odometric position with the true position at 50, 100, and 150 cm. The results obtained for 50 trials are shown in Fig. 2.

The crosses represent the positions given by the odometer and the horizontal line is the true trajectory. The ellipses represent the margins of uncertainty, which include 90%

https://doi.org/10.1017/S0263574708004773 Published online by Cambridge University Press

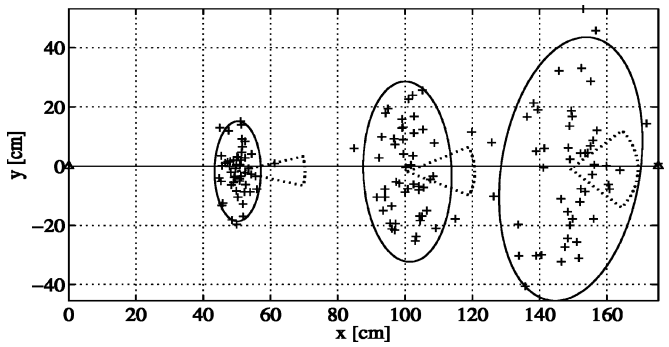

Fig. 2. Tests of the odometry on the VAHM.

of the points, supposing the error vector is governed by a Gaussian model. Table I gives the estimated average and standard deviation of the position and orientation errors at 50, 100, and 150 cm.

For 50 cm covered, the ellipse of uncertainty has a radius of approximately 8 cm on x-axis and 17 cm on y-axis and the error in orientation is about 10°. The drift is faster on the axis orthogonal to the trajectory than on the direction of the trajectory. This is due to the inaccuracy on the orientation which has more repercussions on the orthogonal axis; indeed for a rather small angle the cosine remains almost equal to 1 while the sine is approximately equal to the angle itself. That is why the position estimated in the direction of displacement, proportional to the cosine, varies less with the angle than the position estimated in the orthogonal direction.

As the VAHM project vehicle is intended to move in indoor environments like an apartment or a hospital, a precise estimate of the position is necessary in order to follow the programmed trajectories properly. In this context a position error of 5 cm on each axis and an orientation error of 3° are the limits which we estimate acceptable to ensure the displacement is properly carried out. The results obtained with the odometry show the need for using other sensors so as to get an estimation of the position within the required margins.

4. Contribution of the Ultrasonic Sensors

A belt of 16 ultrasonic sensors is attached to the wheelchair and their measurements are used for other modules such as obstacle avoidance and wall following. We use the data to adjust the position of the wheelchair in relation to its known environment.

4.1. Modeling of measurements and environment

The model of measurements we have defined is a punctual model. We consider that a measurement d perceived by the sensor represents an obstacle located at the distance d from the sensor in its axis (Fig. 3). This model corresponds to reality when the perceived segment is orthogonal with the acoustic axis of the sensor but constitutes a rather strong approximation when the obstacle is orientated differently. The choice of this model is guided by two considerations:

- The punctual model is the lightest to treat during position adjustment and makes it possible to limit execution time.
- Placing the impact point at this location is the means of minimizing modelization errors.

Table I. Error on the odometric position.

	ε_x (cm)		ε_y (cm)		ε_θ (cm)	
Distance	μ	σ	μ	σ	μ	σ
50 cm	0.2	3.2	−1.7	7.9	0.2	4.8
100 cm	0.7	6.1	−1.9	14.2	0.6	8.0
150 cm	−0.8	9.9	−0.9	20.8	−0.2	13.5

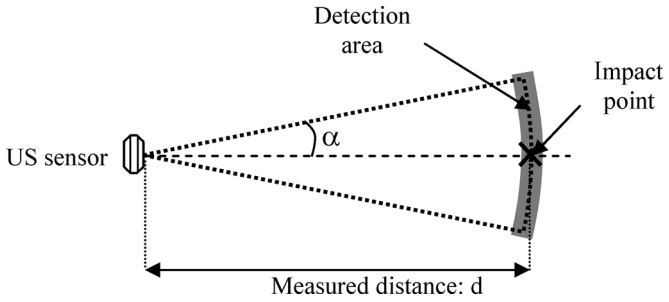

Fig. 3. Punctual model of a US measurement.

From the position and orientation of each sensor on the wheelchair, the location of each impact point is computed in the reference frame linked to the wheelchair. This set of points constitutes the local map of measurements.

The environment in which the robot moves is represented by a set of straight-line segments corresponding to the boundaries between free space and occupied space in the horizontal plane of ultrasonic sensors. An ellipse is associated with each segment; it defines a zone of validity to associate the impact points of the sensors to the segments of the environment. According to the estimation of the errors on the odometric positions (Fig. 2) we take 15 cm for the length of the orthogonal axis of the ellipse. This set of ellipses and segments constitutes the global map of the environment. Figure 4 shows an example of the local map built around the wheelchair in the global map of the environment.

4.2. Matching points and segments

Matching the points of the local map, projected around the current position, and the segments of the global map is achieved according to the following criteria:

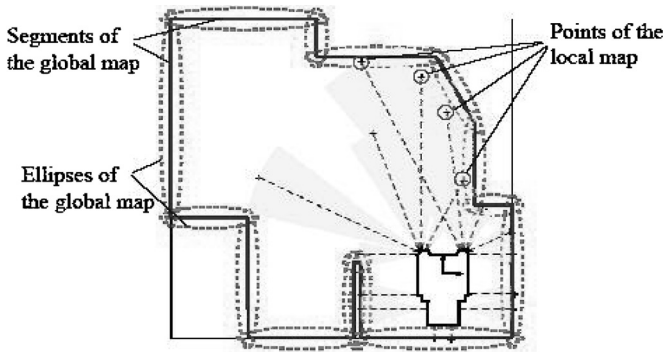

Fig. 4. Local map and global map.

https://doi.org/10.1017/S0263574708004773 Published online by Cambridge University Press

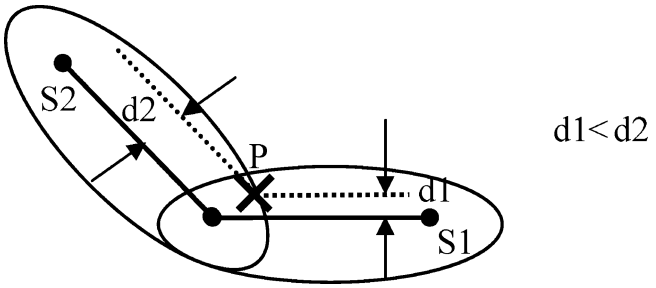

Fig. 5. Multiple matching.

- *Ellipse*: The first condition to assign a point to a segment is that it is located inside the ellipse associated to the segment (see Fig. 4).
- *Angle of incidence*: With ultrasonic sensors, if the wave collides with the obstacle with large angle of incidence, the reflected wave does not return to the sensor and the obstacle is not perceived. Consequently, a matching is validated if the angle of incidence is lower than α (half of the sensor's opening angle).
- *Crosstalk*: In some cases, the wave perceived by a sensor was emitted by another sensor; therefore the measurement of the time of flight is erroneous and represents a fictitious obstacle. A procedure was developed named Error Eliminating Rapid Ultrasonic Firing (EERUF)[30] to avoid this failure of US sensors but it supposes to activate the sensors in a specific mode. In our context the only problem is the risk of a parasitic matching if the fictitious obstacle is confused with a true obstacle in the environment. This type of error can be detected if there is another obstacle between the sensor and the "perceived" segment, proving the unlikelihood of the measurement. Thus, for each matching, we check that there is no obstacle in the path of the ultrasonic wave. If there is, the measurement is aberrant and we eliminate it.
- *Distance criterion*: An impact point may be simultaneously located in two ellipses. If other tests (angle of incidence and crosstalk) are positive in both cases, then we choose the segment closest to the point. In Fig. 5, $d1 < d2$ and therefore point P is associated with segment S1.

After having passed all these tests, each point of the local map is affected with a segment or eliminated if no valid segment is found.

4.3. Method to find the wheelchair's position

The wheelchair's position is determined by calculating the best match between the local map and the global map. First, we select the points on the local map which satisfy the matching conditions described above once projected onto the global map around the current position. Then we determine the translation and the rotation to be applied to the wheelchair's position in order to adjust the points on the segments.[29] The algorithm (Fig. 6) is initialized by the odometric position that is adjusted in an iterative way by calculating several successive translations (T_x, T_y) and rotations (T_Θ). The procedure is repeated until the adjustment obtained is smaller than the acceptable uncertainty, that is to say 5 cm in position and 3° in orientation.

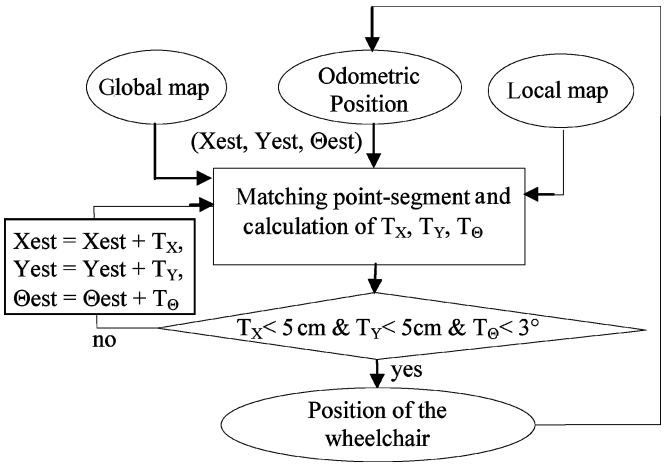

Fig. 6. Localization principle.

4.4. Calculation of the adjustment

The adjustment of the position aims at placing each point P_i from the local map on its associated segment on the global map. That is to say that the displacement of point (x_{pi}, y_{pi}), linked to the adjustment of the position, must cover distance d_i separating the point from the segment.[21] This is expressed by

$$-d_i = [\sin\alpha_i - \cos\alpha_i]\left[T_\theta \begin{pmatrix} 0 & -1 \\ 1 & 0 \end{pmatrix} \begin{pmatrix} x_{p_i} \\ y_{p_i} \end{pmatrix} + \begin{pmatrix} T_x \\ T_y \end{pmatrix}\right](e_i),$$

with α_i being the orientation of the considered segment, T_θ the angle of adjustment in orientation, T_x the adjustment on the x-axis, and T_y the adjustment on the y-axis.

This equation (e_i) supposes that T_θ is sufficiently small to consider that $\sin T_\theta \cong T_\theta$ and $\cos T_\theta \cong 1$; it is defined for each one of Np points on the local model and makes it possible to determine the values of T_x, T_y, and T_θ. Thus, we have Np equations to calculate three unknowns. It is an overdetermined system, which we treat by the least-squared method. It does not ensure that the points will be placed on the segments but it minimizes the sum of the point-to-segment distances squared.

Let us consider vector Y of Np rows and matrix X of Np rows and three columns, with

$$Y_i = -d_i;\ X_{i,1} = \sin\alpha_i;\ X_{i,2} = -\cos\alpha_i;\ \text{and}$$
$$\mathrm{X}_{i,3} = (\cos\alpha_i \ \ \sin\alpha_i) \begin{pmatrix} 0 & -1 \\ 1 & 0 \end{pmatrix} \begin{pmatrix} x_{p_i} \\ y_{p_i} \end{pmatrix}.$$

If

$$b = \begin{pmatrix} T_x \\ T_y \\ T_\theta \end{pmatrix},$$

the system of Np equations (e_i) is expressed by $\mathrm{Y} = \mathrm{X}b$ and the solution $\widehat{b}$ is defined with the least-squared method by $\widehat{b} = (\mathrm{X}^T\mathrm{X})^{-1}\mathrm{X}^\mathrm{T}\mathrm{Y}$. We must have at least three points on the local map to apply this procedure.

https://doi.org/10.1017/S0263574708004773 Published online by Cambridge University Press

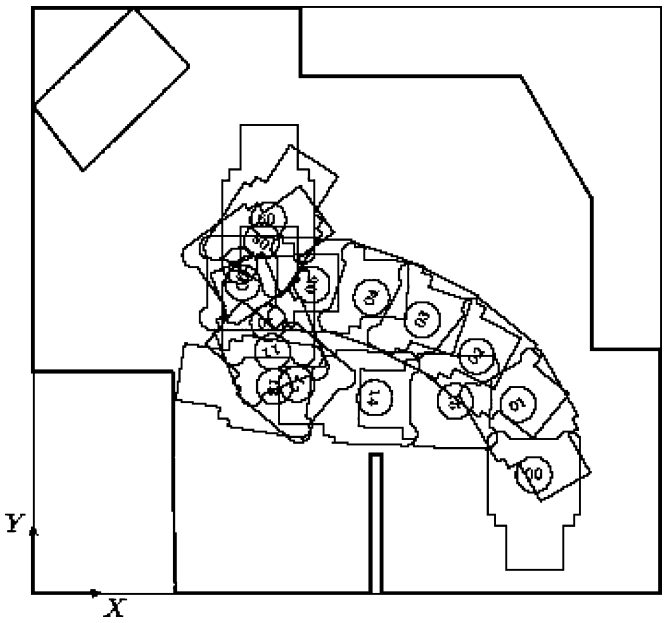

Fig. 7. Trajectory of tests of the adjustment algorithm.

4.5. Tests

We realized a series of tests on the adjustment algorithm on the VAHM prototype in an indoor environment. The 16 positions successively tested are represented in Fig. 7. For each one of them we recorded the values given by the algorithm as well as the position and the orientation of the robot measured on the floor.

The tests are carried out off-line by initializing the odometric position in a set of values located around the true location of the wheelchair, in a square of 30 cm per side and for an orientation in a cone of 20°. The variation step is 1 cm in position and 1° in orientation which leads to testing 20,181 initial positions for one actual position of the vehicle. Table II shows the averages and the standard deviations of the errors on adjusted positions. The processing time is 300 ms on average.

In this table the suppressed rows (1, 2, 8, and 12) correspond to configurations for which the adjustment did not take place because less than three US measurements were associated with line segments from the environment, which is insufficient to carry out the algorithm. In case 3 the adjustment did not work on the x-axis because the sensors did not detect any usable obstacles in that direction. In general the problems appear in the configurations where the positions of the sensors are such that the angle of incidence is large and the approximation of the punctual model very rough, which places the measurement out of the ellipse associated with the segment. But when enough matches are available and most of them are favorable to the punctual model, the error on the estimated position is within the acceptable limits (inferior to 5 cm). On the other hand, we note that the results are not acceptable for the orientation correction: the error is around 7°, which is far above the 3° we were aiming for.

Table II. Errors of localization for the tests.

	ε_x (cm)		ε_y (cm)		ε_θ (°)	
Case	μ	σ	μ	σ	μ	σ
0	0.3	0.3	2	0.4	1.8	2.8
3			2.7	1	7.8	6.9
4	3.1	1.5	1.2	0.7	22.5	12.5
5	2.1	1.7	1.0	0.8	9.8	6.5
6	2.5	0.4	1.3	1.3	8.1	6.5
7	1.3	1.1	1.5	0.6	5.1	4.5
9	3.3	1.2	1.6	0.7	6.4	6.2
10	2	1.2	0.7	0.4	5.5	5.5
11	1.2	0.6	1.7	1.8	2.8	3.6
13	2.3	0.7	0.9	0.4	9.4	11
14	0.5	0.8	0.4	0.7	9.8	5.5
15	1.5	1.5	0.9	0.4	8.4	6.9

Fig. 8. Image of the camera and extracted vertical edges.

The adjustment algorithm performs well on position when a sufficient number of measurements are exploitable. But the correction of the orientation does not significantly improve the results due to the uncertainties on the direction of ultrasonic measurements. The vision sensor that gives another perception of the environment will compensate for this deficiency.

5. Perception of the Orientation Through Vision

5.1. Principle

The camera allows to refine the orientation of the vehicle by watching the vertical boundaries of the environment (edge of blackboard, door, window, etc.) whose position has been recorded beforehand.

Therefore, the first task is to extract the vertical edges of the picture (Fig. 8). To do this the contrast of the picture is enhanced using histogram equalization after which we apply a Deriche filter. The filter is designed to consider only the transitions in the x-axis representing the vertical edges.[21] The filtering result is treated by local non-maxima suppression, hysteresis thresholding, and edge following. Finally we register the x-coordinate of each vertical edge in the picture. The principle of the orientation adjustment is as follows (Fig. 9): knowing the position of a vertical boundary V in the environment and the position of the camera F as well as its estimated orientation $\hat{\theta}_F$, we assess the x-coordinate P where the vertical edge should be seen in the image plan. Then the adjustment τgn the orientation of the camera is determined by the deviation between P and P', where the edge is actually seen.

To associate vertical boundary V with point P' in the picture, the correspondence between the verticals of the environments and the edges detected in the picture must

https://doi.org/10.1017/S0263574708004773 Published online by Cambridge University Press

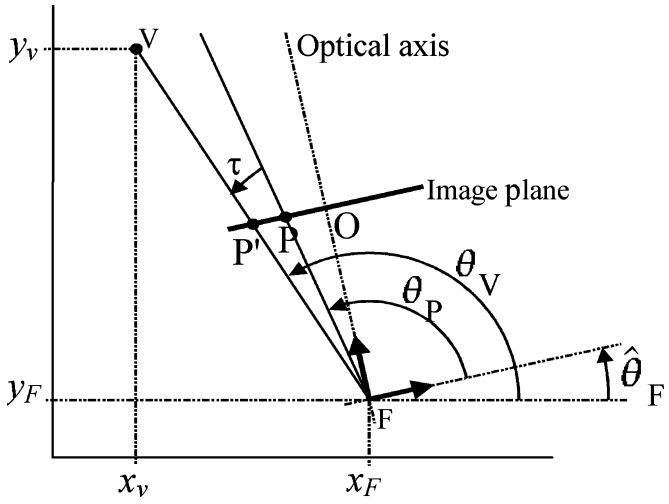

Fig. 9. Adjustment of the orientation of the camera.

be established. To achieve this, we use an interpretation tree which is described in the following subsection.

5.2. *Interpretation tree*

The interpretation tree is a structure, created in a recursive way, which establishes all the possible correspondences between the edges of the picture and the verticals of the environment. From a root R each level represents an edge and each node represents a pairing between this edge and one of the possible verticals. Figure 10 shows an example of a tree created for two edges and four verticals.

For each node, an adjustment τ of the camera's orientation is calculated according to the principle described above. The branch, which represents the proper matching of the M edges with the N verticals, will have appreciably constant values of τ along its successive nodes. Thus, we calculate the average and the standard deviation of the successive adjustments of the branches. The correct matching is detected by searching for the branch with the smallest standard deviation. And the estimated value of the adjustment is the average value of this branch.

5.3. *Refinement of the tree*

Limitation of the verticals: To reduce the dimension of the tree and the time necessary for its analysis, we consider only part of the verticals of the environment. We select those that are in the camera's field of vision widened with a 10° angular margin to account for the uncertainty on its orientation. Then we eliminate the verticals hidden by an obstacle (Fig. 11).

Pruning of the tree: In the initial tree all possible combinations of M edges with N verticals are considered. But

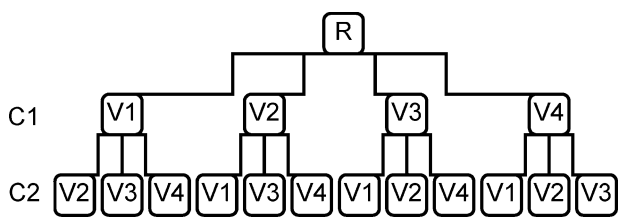

Fig. 10. Interpretation tree for two edges and four verticals.

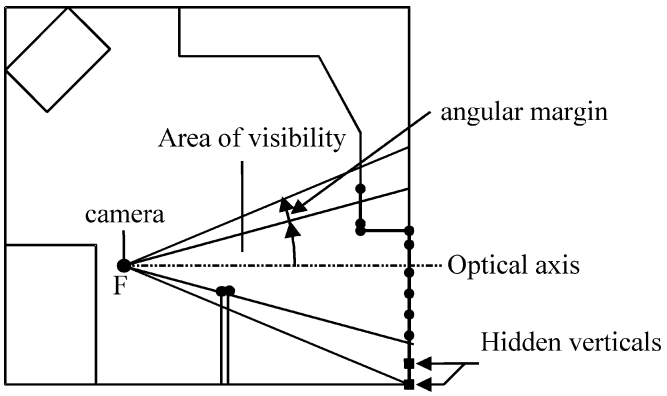

Fig. 11. Selection of the verticals.

some solutions are not coherent in so far as they "cross" projections. For example in the case of Fig. 12 if edge Cb is associated with vertical V2 then, at the inferior level of the tree, edge Cc cannot be associated with vertical V1.

This matching analysis considerably reduces the size of the tree[21]; indeed if we value S_t, the number of nodes in the initial tree for M edges and N verticals, we obtain

$$S_{\mathrm{t}} = \sum_{i=1}^{M} A_N^i = \sum_{i=1}^{M} \frac{N!}{(N-i)!}.$$

If we consider S_e the same number for the pruned tree, we obtain

$$S_{\mathrm{e}} = \sum_{i=1}^{M} C_N^i = \sum_{i=1}^{M} \frac{N!}{i!(N-i)!}$$

because the order in which the verticals are treated no longer matters. In fact, the place of the edges in the picture imposes the verticals they are associated to. For example, for nine verticals and five edges, the total tree has 18,729 nodes but this number is reduced to 381 for the pruned tree, that is to say 50 times fewer.

Introduction of "nil nodes": The first tests carried out showed that the presence of parasitic edges could deteriorate the matching procedure. Indeed, the mode of creation of the tree, where each level represents an edge, imposes the association of the edge with a vertical to consider the next edge. Therefore a parasitic edge will be associated to a vertical which cannot be used thereafter, which ruins the procedure. To overcome this problem we create a "nil node" which associates a given edge from the picture to a virtual vertical. This vertical does not exist in the environment but

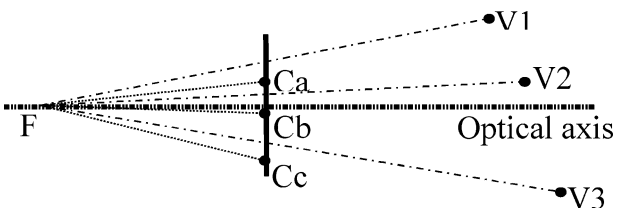

Fig. 12. Coherence of matching vertical-edges.

https://doi.org/10.1017/S0263574708004773 Published online by Cambridge University Press

Table III. Errors corrected in orientation.

Case	ε_x (cm)	ε_y (cm)	$\varepsilon_{\theta\min}$ (°)	$\varepsilon_{\theta\max}$ (°)
0	5	5	−20	21
1	5	5	−14	9
2	7	5	−17	19
3	9	10	−15	23
4	8	5	−17	16
5	5	11	−2	10
6	10	5	−14	11
7	6	5	−10	10
8	6	8	−12	14
9	9	8	−10	19
11	8	7	−12	18
12	9	10	−12	11
13	7	8	−10	10
14	5	8	−20	17
15	8	8	−10	18

it is treated like any other vertical, which neutralizes the influence of a parasitic edge on the construction of the tree.

5.4. Tests on the prototype

In order to test the performances of the procedure, we go back to the 16 successive positions of the wheelchair used for the previous tests (Fig. 7). We define a position of the wheelchair its true position to which we add a random error ranging between 5 and 11 cm. And we estimate the error range on the orientation that can be corrected by the vision. That is to say that we increase the initial value of the error until we reach the limit for which the procedure does not deliver a correct orientation to within 3°. In Table III, position errors are in the left columns and the ranges of orientation error are given in the two right-hand-side columns.

The procedure proves to be operational in most cases except in trials 5 and 10. For trial 10 the procedure could not be carried out because only one edge is present in the picture. For trial 5 the inferior limit is –2° because the position error is large on y-axis (11 cm) which puts several edges into the picture which do not correspond to selected verticals from the model. But in general the range of acceptable errors exceeds $\pm 10°$ which is consistent with our expectations since the orientation error is in this range after US adjustment.

The procedure described here uses vision as a complementary mode of perception so as to adjust the orientation of the vehicle. It is based on the matching of vertical edges perceived in the picture and known vertical segments of the environment. The calculation charge inherent in this type of approach is limited because we select the verticals located in the camera's field of vision and take topological criteria into account to consider possible matches. We obtain an algorithm which is carried out in a mean time of 500 ms and which gives acceptable results in most cases.

6. Conclusion

The work reported in this paper explores the possibilities of localization, during movement, of our prototype in its environment. We established a mode of adjustment of the odometric position using ultrasonic sensors and vision, which, under certain conditions, give the position of the wheelchair in less than 1 s. The difficulty to compare the performances of our method with those reported in the technical literature is the specificity of our application. We know the method of localization with odometry (Borenstein), US sensors (Crowley), vision (Krotkov), or fusing several sensor measurements (Thrun), but the specificity of our work is the search of a simple way to fuse the measures of different sensors in order to apply it in the field of the mobility aid for people with disabilities. The differences between the contexts makes the comparison uneasy.

Moreover, we discuss the result obtained by off-line implementation of our approach because with the on-line implementation we could not assess the deviation between the values given by the algorithm and the true values of the position and the orientation of the wheelchair. We chose to detail every step of the trajectory in order to specify the propitious cases for the procedure. Yet the on-line tests are in progress in our laboratory. The use of this procedure, in actual conditions, requires a possible intervention of the user, in order to signal if a failure occurs. In this case the wheelchair stops and static localization is carried out.

Like most of the projects initiated in the nineties, at first the VAHM project sought to adapt mobile robotics methods to driving assistance for electrical wheelchairs. Rehabilitation robotics now tends to aim for a closer cooperation between the user and the intelligent wheelchair. Thus, the VAHM project is heading toward a more reactive approach of displacements. Therefore, the context of a totally modeled environment and the "trajectory execution" mode are called into question. However, the undertaken study makes it possible to specify the fields of efficiency of each sensor and to consider how to make the most of the complementarity of their perception capabilities.

References

1. A. Argyros, P. Georgiadis, P. Trahanias and D. Tsakiris, "Semi-autonomous navigation of a robotic wheelchair," *J. Intell. Robot. Syst.* **34**, 315–329 (2002).
2. D. P. Miller and M. G. Slack, "Design and testing a low-cost robotic wheelchair prototype," *Autonomous Robot*, **2**, 77–88 (1995).
3. H. A. Yanko, Shared User-Computer Control of a Robotic Wheelchair System *Ph.D. Thesis* (Department of Electrical Engineering and Computer Science, Massachusetts Institute of Technology, University of Massachusetts, Lowell, Sep. 2000).
4. R. Simpson, E. LoPresti, S. Hayashi, I. Nourbakhsh and D. Miller, "The smart wheelchair component system," *J. Rehabil. Res. Dev.* **41**(3B), 429–442 (Jun. 2004).
5. J. Borenstein and L. Feng, "Measurement and correction of systematic odometry errors in mobile robots," *IEEE Trans. Robot. Automation* **12**(6), 869–880 (Dec. 1996).
6. I. Moon, S. Joung and Y. Kum, "Safe and Reliable Intelligent Wheelchair Robot With Human Robot Interaction," *Proceedings of the IEEE International Conference on Robotics and Automation*, Washington (May 2002) pp. 3595–3600.
7. S. P. Levine, D. A. Bell, L. A. Jaros, R. C. Simpson, Y. Koren, "The NavChair assistive wheelchair navigation system," *IEEE Trans. Rehabil. Eng.* **7**(4), 443–451 (Dec. 1999).
8. G. Del Castillo, Autonomous, Vision-Based, Pivoting Wheelchair With Obstacle Detection Capability *Ph.D. Thesis* (University of Notre Dame, Notre Dame, Indiana, USA, May 2004).

https://doi.org/10.1017/S0263574708004773 Published online by Cambridge University Press

9. R. C. Luo, T. M. Chen and M. H. Lin, "Automatic Guided Intelligent Wheelchair System Using Hierarchical Grey-Fuzzy Motion Decision-Making Algorithms," *Proceedings of the IEEE/RSJ International Conference on Intelligent Robots and Systems*, Kyongju, Korea (1999) pp. 900–905.
10. G. Pires and U. Nunes, "A wheelchair steered through voice commands and assisted by a reactive fuzzy-logic controller," *J. Intell. Robot. Syst.* **34**, 301–314 (2002).
11. A. Bonci, S. Longhi, A. Monteriu and M. Vaccarini, "Navigation system for a smart wheelchair," *J. Zhejiang Univ. Sci.* **6A**(2), 110–117 (2005).
12. T. Gomi and A. Griffith, "Developing Intelligent Wheelchairs for the Handicapped," **In**: *Assistive Technology and Artifical Intelligence* (V. O. Mittal, H. A. Yanco, J. M. Aronis, R. C. Simpson, eds.) (Springer Verlag, 1998) pp. 150–178.
13. E. Demeester, M. Nuttin, D. Vanhooydonck and H. Van Bruusel, "A Model-based, Probabilistic Framework for Plan Recognition in Shared Wheelchair Control: Experiments and Evaluation," *Proceedings of the IEEE/RSJ International Conference on Intelligent Robots and Systems* 2003, Las Vegas, USA, pp. 1456–1461.
14. Y. Kuno, Y. Murakami and N. Shimada, "User and Social Interfaces by Observing Human Faces for Intelligent Wheelchairs," *ACM International Conference, Proceeding of Workshop on Perceptive User Interfaces*, Orlando, Florida, USA (2001) pp. 1–4.
15. A. Lankenau, T. Rofer and B. Krieg-Bruckner, "Self localization in large-scale environments for the Bremen autonomous wheelchair," *Spatial Cognition III*. Lecture Notes in Artificial Intelligence 2685, 2003, pp. 34–61.
16. Y. Adachi, H. Tsunenari, Y. Matsumoto and T. Ogasawara, "Guide Robot's Navigation Based on Attention Estimation Using Gaze Information," *Proceedings of the IEEE/RSJ International Conference on Intelligent Robots and Systems*, Sendai, Japan (2004) pp. 540–545.
17. C. Zhou, Y. Wei and T Tan, "Mobile Robot Self-Localization Based on Global Visual Appearance Features," *Proceedings of the IEEE International Conference on Robotics and Automation*, Taipei, Taiwan (2003) pp. 1271–1276.
18. S. V. Diaz, C. A. Rodriguez, F. Diaz del Rio, A. C. Balcells and D. C. Muniz, "Tetranauta: A Intelligent Wheelchair for Users with very Severe Mobility Restrictions," *Proceedings of the International Conference on Control Applications*, Glasgow, Scotland UK. (2002) pp. 778–783.
19. J. C. G. Garcia, M. M. Romera, M. M. Quintas and J. U. Urena, "Positioning and Localization System for Autonomous Wheelchairs," *Proceedings of the IEEE Industrial Electronics Society*, Orlando, Florida, USA (Nov. 2002) pp. 1555–1560.
20. G. Bourhis, O. Horn, O. Habert and A. Pruski, "The VAHM project: Autonomous vehicle for people with motor disabilities,"*IEEE Robot. Automation Mag.,* Special Issue on Wheelchairs in Europe **7**(1), 21–28 (Mar. 2001).
21. M. Kreutner, Perception multisensorielle pour véhicule autonome dédié aux personnes handicapées moteurs *These de doctorat de l' Université de Metz*, University of Metz, France (Sep. 2004).
22. P. Hoppenot and E. Colle, "Real-time localisation of a low-cost mobile robot with poor ultrasonic data," *IFAC J. Control Eng. Pract.* **6**, 925–934 (1998).
23. C. H. Kim, J. H. Juang and B. K. Kim, "Design of an Intelligent Wheelchair for the Motor Disbled," **In**: *Advances in Rehabilitation Robotics, Lecture Notes in Control and Information Sciences* (Z. Z. Bien and Stefanov, eds.) (Springer Berlin/Heidelberg 2004) pp. 299–310.
24. L. Jetto, S. Longhi and G. Venturini, "Development and experimental validation of an adaptive extended kalman filter for the localization of mobile robots," *IEEE Trans. Robot. Automation* **15**(2), 219–229 (Apr. 1999).
25. K. Schilling, H. Roth, R. Lieb and H. Stuzle, "Sensors to Improve the Safety for Wheelchair Users," *Proceedings of the 3*rd *Annual TIDE-Technology for Inclusive Design and Equality-Congress, 1998*, Helsinki, Finland, pp. 327–331.
26. W. S. Gribble, R. L. Browning, M. Hewett, Emilio Remolina and B. J. Kuipers, "Integrating Vision and Spatial Reasoning for Assistive Navigation," **In**: *Assistive Technology and Artifical Intelligence* (V. O. Mittal, H. A. Yanco, J. M. Aronis, R. C. Simpson, eds.) (Springer Verlag, 1998).
27. O. Horn and A. Courcelle, "Interpretation of ultrasonic readings for autonomous robot localization," *J. Intell. Robot. Syst.* **39**, 265–285 (2004).
28. P. Mallet and J. M. Pergandi, "Towards smart wheelchairs," *AAATE 2005*, Lille, France, pp. 328–335.
29. M. Kreutner and O. Horn, "Co-operation between ultrasound and monocular vision for the localization of a mobile robot," CESA'2003, Lille, France (2003).
30. J. Borenstein and Y. Koren, "Noise Rejection for Ultrasonic Sensors in Mobile Robot Application," *Proceedings of the IEEE International Conference on Robotics and Automation*, (Aut 1992) pp. 1727–1732.

https://doi.org/10.1017/S0263574708004773 Published online by Cambridge University Press